Green Chemistry

Cutting-edge research for a greener sustainable future

rsc.li/greenchem

ROYAL SOCIETY
OF **CHEMISTRY**
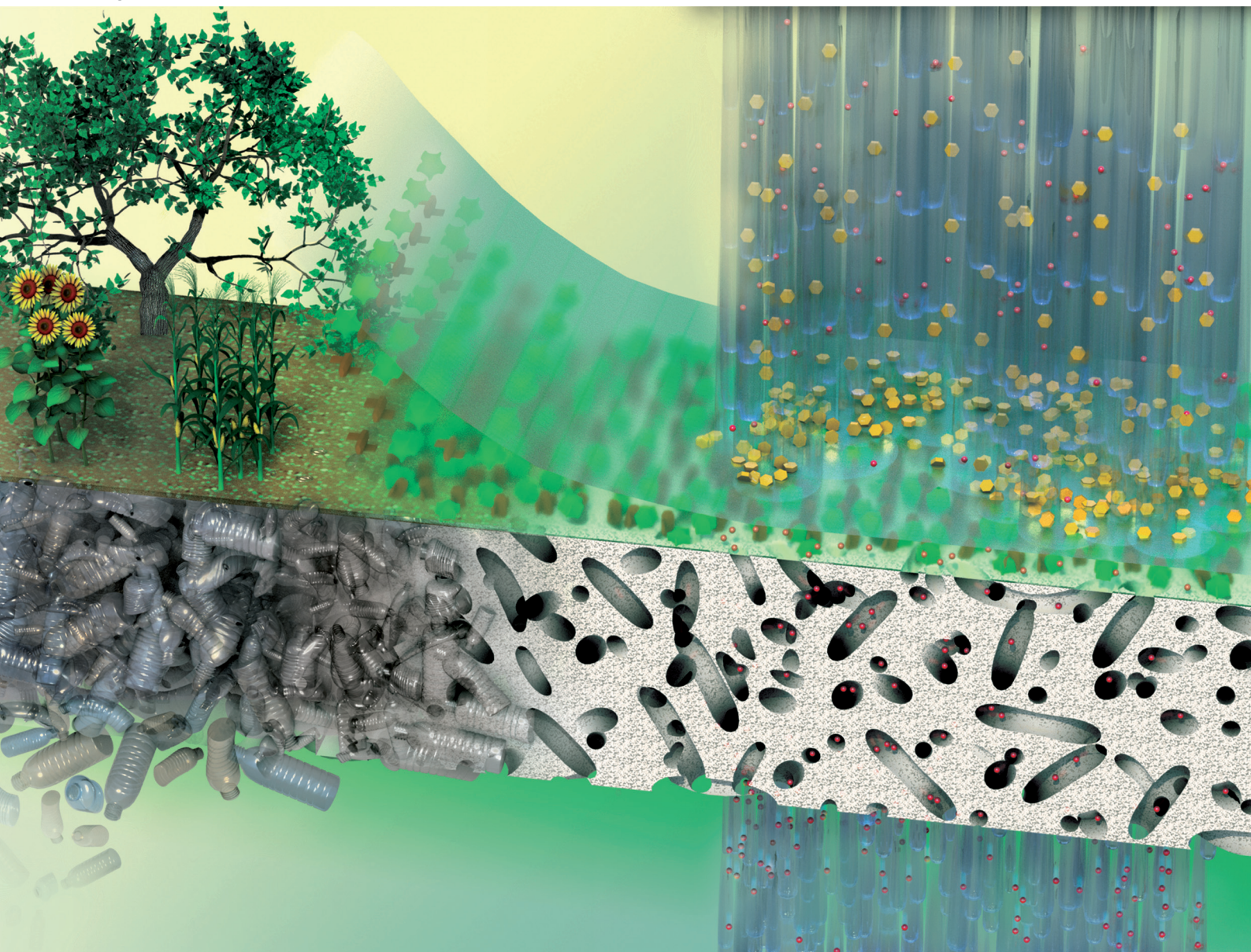
PAPER
Gyorgy Szekely *et al.*
Hydrophobic thin film composite nanofiltration membranes
derived solely from sustainable sources

Check for updates

Hydrophobic thin film composite nanofiltration membranes derived solely from sustainable sources†

Sang-Hee Park, [ID] [a] Abdulaziz Alammar, [ID] [b] Zsolt Fulop, [ID] [a] Bruno A. Pulido, [ID] [c] Suzana P. Nunes [ID] [c] and Gyorgy Szekely [ID] *[a,b]

Membrane separations are considered to be sustainable technologies because of their relatively low energy consumption. However, the fabrication of membranes is yet to turn green. Thin film composite (TFC) membranes are fabricated from petroleum-based monomers and solvent systems, which can undermine the energy-saving benefits of their application in separation processes. Here, we report high-performance TFC membranes fabricated solely from sustainable resources such as plant-based monomers (priamine, tannic acid), green solvents (*p*-Cymene, water) and recycled polymer waste (PET). We found that the ultrathin selective layer (30 nm) of the hydrophobic membrane exhibited excellent performance, and an acetone permeance as high as 13.7 L m^{-2} h^{-1} bar^{-1} with a 90% rejection of styrene dimer (235 g mol^{-1}). Stability in six solvents and long-term continuous nanofiltration over one week demonstrated the robustness of the membranes. Control over the selectivity of the membrane (cut-off between 236 and 795 g mol^{-1}) was successfully achieved by changing the conditions of the interfacial polymerization.

Introduction

The potential of membranes for energy-efficient separations has long been recognized, albeit slowly realized. From a technology viewpoint, membranes provide a sustainable solution for separations, which account for 10–15% of the global consumption of energy. There has been a significant effort to develop novel membrane materials that can achieve separations faster and more selectively. However, most of the existing methodologies use petrochemical-based monomers, polymers and toxic solvents. Tackling the sustainability issues of membrane materials and membrane fabrication is an emerging area of research. Recent efforts in biomass conversion resulted in the availability of new building blocks and solvents, which can potentially be used for preparing membranes.

[a]Advanced Membranes and Porous Materials Center, Physical Science and Engineering Division (PSE), King Abdullah University of Science and Technology (KAUST), Thuwal, 23955-6900, Saudi Arabia. E-mail: gyorgy.szekely@kaust.edu.sa; http://www.szekelygroup.com
[b]Department of Chemical Engineering & Analytical Science, School of Engineering, The University of Manchester, The Mill, Sackville Street, Manchester, M1 3BB, UK. E-mail: gyorgy.szekely@manchester.ac.uk
[c]Advanced Membranes and Porous Materials Center, Biological and Environmental Science and Engineering Division (BESE), King Abdullah University of Science and Technology (KAUST), Thuwal, 23955-6900, Saudi Arabia
†Electronic supplementary information (ESI) available. See DOI: 10.1039/d0gc03226c

Thin film composite (TFC) membranes, consisting of an ultrathin selective layer (less than 50 nm), often on top of a porous polymer support (approx. 100 μm), have been extensively used in diverse separation processes, due to their high permeance and permselectivity, excellent chemical and physical stability.[1,2] In particular, solvent-resistant TFC membranes for organic solvent nanofiltration (OSN) were first reported by Livingston *et al.* almost a decade ago.[3] Those TFC membranes are fabricated with an ultrathin polyamide selective layer on a crosslinked polyimide porous support *via* interfacial polymerization (IP) of *m*-phenylenediamine (MPD) and trimesoyl chloride (TMC). At the end of the IP reaction, unreacted amine and acyl chloride groups remain in the polyamide selective layer.[4] In addition, the undesired hydrolysis of unreacted acyl chloride groups takes place due to the presence of the aqueous MPD solution.[5] This side-reaction results in the formation of carboxylic acid groups in the selective layer.[6] The unreacted amine and the converted carboxylic acid moieties endow the membrane with a hydrophilic nature. These membranes exhibit high permeance for hydrophilic solvents and low permeance for hydrophobic solvents. The latter solvents are often used in the pharmaceutical, paint and petrochemical industries on a large scale. Therefore, there is a need to develop different strategies to obtain hydrophobic membranes that are suited for separations in non-polar solvents as well as their recovery.

A few studies on the fabrication of hydrophobic TFC membranes have been reported.[7–10] For example, monoacyl chlor-

ide- and monoamine-functional monomers containing fluorine groups were used as co-monomers with MPD and TMC to enhance the hydrophobicity of the selective layer.[7,8] These membranes exhibited a water contact angle higher than 90°, which improved their permeance for non-polar solvents without sacrificing their selectivity. The molecular weight cut-off (MWCO) remained approximately 235 g mol⁻¹ but the obtained permeance was still very low (0.3 L m⁻² h⁻¹ bar⁻¹). Zhang et al.[9] recently reported a crosslinked polyacrylonitrile/polyethyleneimine-polydimethylsiloxane TFC membrane, which showed a low swelling property of approx. 3% but this was somewhat offset by the high MWCO (600 g mol⁻¹) and low permeance of 0.4 L m⁻² h⁻¹ bar⁻¹. Photo-curable perfluoropolyether (PFPE) was coated on Matrimid® support cross-

linked with 1,6-hexanediamine, and polymerized by UV irradiation.[10] Until now, the coating of fluorine-based materials has been one of the most promising methods to prepare hydrophobic TFC membranes, albeit their thick and loose selective layer provides a low permeance for both polar and non-polar solvents, despite their high MWCO values of 350–600 g mol⁻¹.

The challenge is multifaceted and lies in finding sufficiently reactive natural monomers that are soluble in green solvents with opposing polarities. On one hand, the monomers need to be reactive to form a highly crosslinked thin film. On the other hand, one of the monomers need to be soluble in polar solvents, while the other monomer need to be soluble in a non-polar solvent, which is immiscible with the
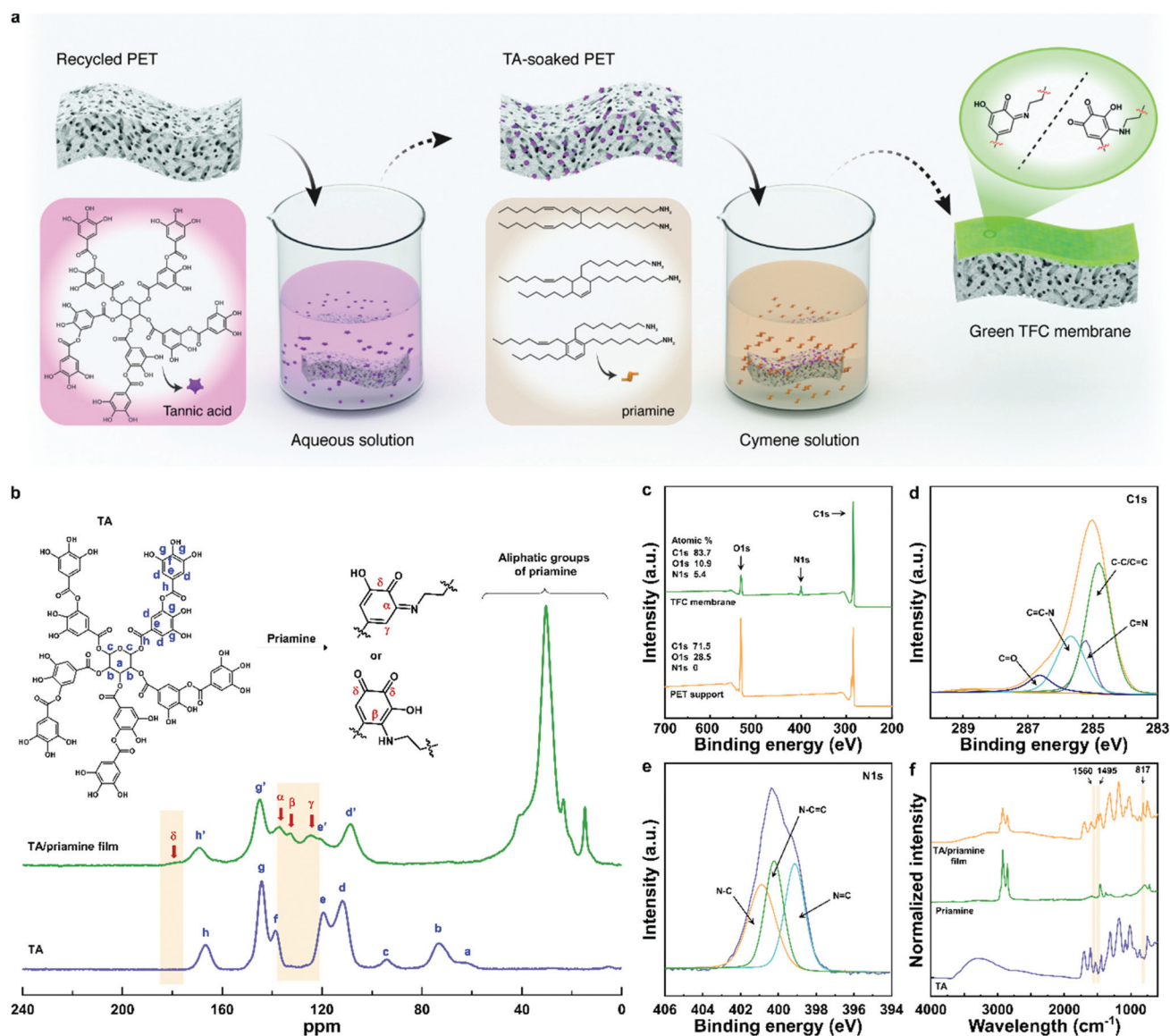

Fig. 1 Membrane preparation and chemical characterization. (a) Fabrication process of a green TFC membrane *via* the IP reaction of priamine and tannic acid (TA); (b) solid-state ¹³C NMR spectra of TA and the TA/priamine free-standing film produced at 0.1 mmol/v% monomer concentrations; (c) wide XPS spectra of the green TFC membrane and recycled PET support, deconvoluted high-resolution (d) C 1s and (e) N 1s peaks, and (f) ATR-FTIR spectra of TA, priamine, and the TA/priamine free-standing film.

selected polar solvent. Here, we used plant-based priamine and tannic acid (TA) monomers in green solvents to develop hydrophobic and solvent-resistant TFC nanofiltration membranes. It is the first time that priamine, which is usually obtained from the fatty acids of vegetable oils (e.g., soybean oil and sunflower oil),[11,12] is used as a curing agent to obtain a crosslinked selective layer through its reaction with tannic acid (TA). The cyclohexane, benzene and aliphatic moieties of priamine are suitable to increase the hydrophobicity of the membrane surface, which in turn can result in the high permeance of non-polar solvents. In addition, TA is a representative polyphenol compound, which can be extracted from a diverse range of natural materials such as trees, plants, nuts and fruits.[13,14] The large number of catechol groups in TA have high reactivity with primary amine groups, leading to the formation of strong, solvent-resistant covalent bonds through the Michael addition and Schiff base reactions.[15,16] Thus, it has been recently used as a monomer for TFC membranes due to their high reactivity and high solubility in water.[13–16,17]

Waste upcycling is gaining attention as a sustainable methodology, giving a second life to waste materials, and can minimize the environmental burden of various industries.[18,19] For example, used plastic bottles made of hydrophobic polyethylene terephthalate (PET) can be recycled into a porous support,[20] and used for interfacial polymerization to obtain the priamine-TA selective layer. Interfacial polymerizations are generally performed in toxic, petrochemical-based solvents such as toluene and hexane. Therefore, we screened green solvents and found a new platform for the fabrication of TFC membranes. p-Cymene, a less toxic solvent recommended by the GSK solvent sustainability guide,[21] was used as the organic phase.

Results and discussion

Membrane design

A chemically stable selective layer was formed on a recycled porous PET support with 7% surface porosity (Fig. S1 and S3†) through the IP reaction of TA and priamine, as shown in Fig. 1a. The support was previously optimized for membrane separations.[20] The pyrogallol groups of TA were converted to quinone moieties, under weak alkaline conditions, allowing a rapid reaction with the amine groups of priamine, via Schiff-base and Michael-addition reactions, finally resulting in the formation of imine (–C=N–) and amine (–C–NH–) groups, respectively (Fig. S2†).[15] To investigate the reaction mechanism, solid-state ^{13}C NMR spectra of TA and the TA/priamine free-standing film were obtained (Fig. 1b). The characteristic peaks of TA were observed at 155–180, 130–155, 105–130, and 40–100 ppm, corresponding to carbonyl, hydroxyl-substituted phenolic, aromatic and cyclo-aliphatic groups, respectively.[22,23] After the formation of the TA/priamine free-standing film, peaks corresponding to the aliphatic groups of priamine were observed below 60 ppm. In parallel, the three peaks corresponding to cyclo-aliphatic groups at 40–100 ppm that were

imparted from the core of TA, disappeared. Moreover, four new peaks designated as alpha (α), beta (β), gamma (γ) and delta (δ) were found at 137, 132, 125, and 179 ppm, respectively. The α peak was attributed to the formation of imine (–C=N–) groups, resulting from the Schiff-base reaction. This reaction also involved the formation of aromatic and carbonyl groups, and led to the respective appearance of the γ and δ peaks in the spectra. In addition, the Michael-addition reaction resulted in the formation of aromatic amine (β) and carbonyl (δ) groups. Additionally, the d′ peak at 108 ppm shifted downfield, e′ peak at 120 ppm, g′ peak at 145 ppm and h′ peak at 169 ppm shifted upfield, due to the film formation; these shifts were attributed to the formation of both aromatic imine and amine groups.[22]

To better understand the reaction mechanism, XPS spectra of the green TFC membrane and recycled PET support, as well as FTIR spectra of TA, priamine and TA/priamine free-standing film were recorded. As a result of the IP reaction, a new N 1s peak appeared and the atomic percentage of C 1s peak significantly increased, which showed the presence of amine groups and long aliphatic chains of priamine on the surface of the membrane, respectively (Fig. 1c). The high-resolution XPS peaks of C 1s and N 1s for the green TFC membrane were deconvoluted to confirm the covalent bonds between TA and priamine. The C 1s spectrum was deconvoluted to four characteristic peaks at 284.4, 285.2, 285.7 and 286.6 eV, corresponding to the C–C/C=C, C=N and C=C–N and C=O peaks, respectively (Fig. 1d). In addition, the C=N, C=C–N and C–N peaks at 399.0, 400.4 and 401.0 eV were deconvoluted from the high-resolution N 1s spectrum (Fig. 1e). All this allowed us to reasonably postulate that the observed imine (C=N) and C=C–N peaks came from the Schiff-base reaction and Michael-addition reaction of TA with priamine, respectively.[15] Moreover, Fig. 1f shows the FTIR spectra, before (priamine and TA monomers) and after (the priamine/TA free-standing film) the IP reaction. A broad peak (2000 to 3700 cm^{-1}) corresponding to the O–H stretching of TA, N–H stretching of priamine and the formation of hydrogen bonding between the O–H and N–H groups was observed, as well as sharp peaks from 2700 to 3000 cm^{-1}, corresponding to the aliphatic C–H stretching of priamine. The new peaks at 817, 1495 and 1560 cm^{-1} observed for the TA/priamine film can be attributed to C–H, C–N and C=N stretching, respectively.[24] We found the new C–N and C=N peaks to be in agreement with the XPS results. Therefore, solid-state ^{13}C NMR and XPS analyses demonstrated that the selective layer was produced on the recycled porous PET support through the Schiff-base reaction and Michael-addition reaction of TA and priamine, leading to the formation of new C–C=N and C=C–N bonds.

Membrane properties

Fig. 2 presents the properties of the green TFC membrane and the recycled porous PET support. The surface and cross-section SEM images of the TFC membrane demonstrate the formation of a flat and ultra-thin selective layer. The large
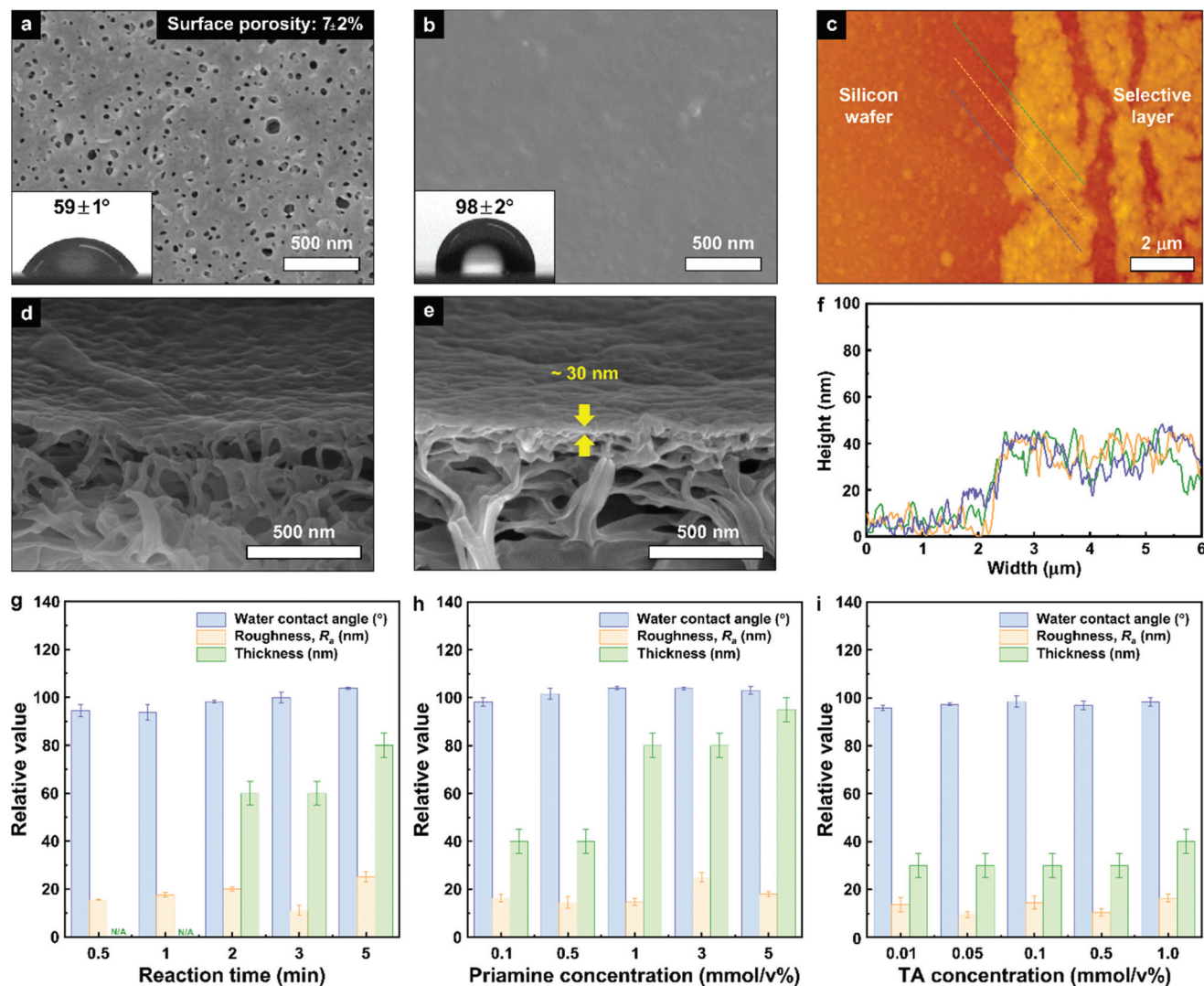
Fig. 2 Morphological and surface characterization. Surface (a and b), and cross-sectional (d and e), SEM images of the recycled PET support (a and d), and the TFC membrane (b and e), as well as AFM height images (c), and their height profile (f), for the free-standing film. The insets represent the digital camera images of the water contact angles. The membranes were fabricated at 0.1 mmol/v% monomer concentrations. Refer to the ESI† for more details on the membrane characterization at other concentrations (Fig. S4–S9†). Water contact angle, roughness (R_a) and thickness of the selective layer for the green TFC membranes prepared under different reaction conditions: (g), reaction time, (h), priamine concentrations and (i), TA concentrations.

number of surface pores observed on the recycled porous PET with a surface porosity of $7 \pm 2\%$ disappeared as a result of the IP reaction. The support has a water contact angle of $59 \pm 1°$, in contrast with the hydrophobic nature of the TFC membrane water contact angle of $98 \pm 2°$ (Fig. 2b). The increase in contact angle also demonstrates the successful incorporation of the long hydrophobic alkyl chains of priamine into the selective layer. These changes contribute to an increase in the adsorption of non-polar solvents at the membrane surface.[25] The thickness of the selective layer (approx. 30 nm), was estimated by both cross-section SEM image (Fig. 2e) and AFM analysis (Fig. 2c and f). In addition to the increase in hydrophobicity, the ultra-thin selective layer also improved the solvent permeance by decreasing the resistance through the membrane.

The hydrophobicity, surface roughness and thickness of a selective layer play a critical role in determining the membrane performance. Therefore, we investigated the correlation between the membrane properties and membrane performance by changing the reaction conditions for the IP (Fig. 2g–i). The results showed that the contact angle between the water and the selective layer slightly increased (from 95° to 104°) as the reaction time increased (Fig. 2g). In addition, as the priamine concentration increased from 0.1 to 1.0 mmol/v%, the water contact angle increased and reached the apex with the value of 104° (Fig. 2h). These results can be attributed to the increase in hydrophobicity of the selective layer, when increasing the amount of long aliphatic chains of priamine with a higher reaction time and priamine concentration. On the

other hand, the significant 100-fold increase in the TA concentration from 0.01 to 1 mmol/v% did not have any significant effect on the water contact angle, which ranged from 95.7° to 98.4° (Fig. 2i). All selective layers exhibited similar flat surfaces with a roughness (R_a) of lower than 25 nm. The roughness and complex morphology of the IP layer is believed to be the result of convection at the aqueous/organic interface. Larger monomers such as those used here have a lower mobility and might contribute to a less convective, more stable interface. The thickness of the selective layers increased with increasing reaction time and priamine concentration (40–95 nm). Similar to the observed trend with the water contact angle, a quasi-constant thickness of the ultrathin selective layer was observed, irrespectively of the TA concentration. Consequently, the fabrication of an ultrathin and hydrophobic selective layer could be achieved at low priamine and TA concentrations, which is expected to improve both the permeance in non-polar solvents, and the sustainability of the membrane.

Membrane performance

To optimize the performance of the green TFC membranes, different reaction conditions such as reaction time and priamine and TA concentrations were employed. The acetone permeance monotonously decreased (Fig. 3a), whereas the polystyrene rejection increased (Fig. 3d) as a result of the increase in reaction time. In addition, the pore size of the membranes sharply decreased from 2.6 to 0.41 nm with an increase in reaction time (Fig. 3b). These results are in line with those obtained for the denser and thicker selective layer formed at higher reaction times (Fig. S4†). The tightest membrane was obtained with an IP reaction time of 5 min, which showed 9.1 ± 0.5 L m⁻² h⁻¹ bar⁻¹ of acetone permeance and a molecular weight cut-off (MWCO) as low as approx. 395 g mol⁻¹. The reaction time was fixed at 5 min for further optimization. Interestingly, the acetone permeance linearly decreased from 16.9 ± 0.6 to 5.7 ± 0.4 L m⁻² h⁻¹ bar⁻¹ with increasing priamine concentration ($y = -2.22x + 16.35$, $R^2 = 0.9743$) (Fig. 3a). Nonetheless, all membranes showed similar MWCO values of approx. 395 g mol⁻¹ and constant pore size of 0.46 nm (Fig. S11 and S12†), indicating the formation of a selective layer with a similar density in the chemical structure (Fig. 3e). Thus, we could conclude that the decrease in acetone permeance was mainly caused by the increase in thickness of the selective layer. The initial increase in TA concentration (from 0.01 to 0.1 mmol/v%) resulted in a 29% reduction of acetone permeance and a gradual decrease in MWCO from 795 to
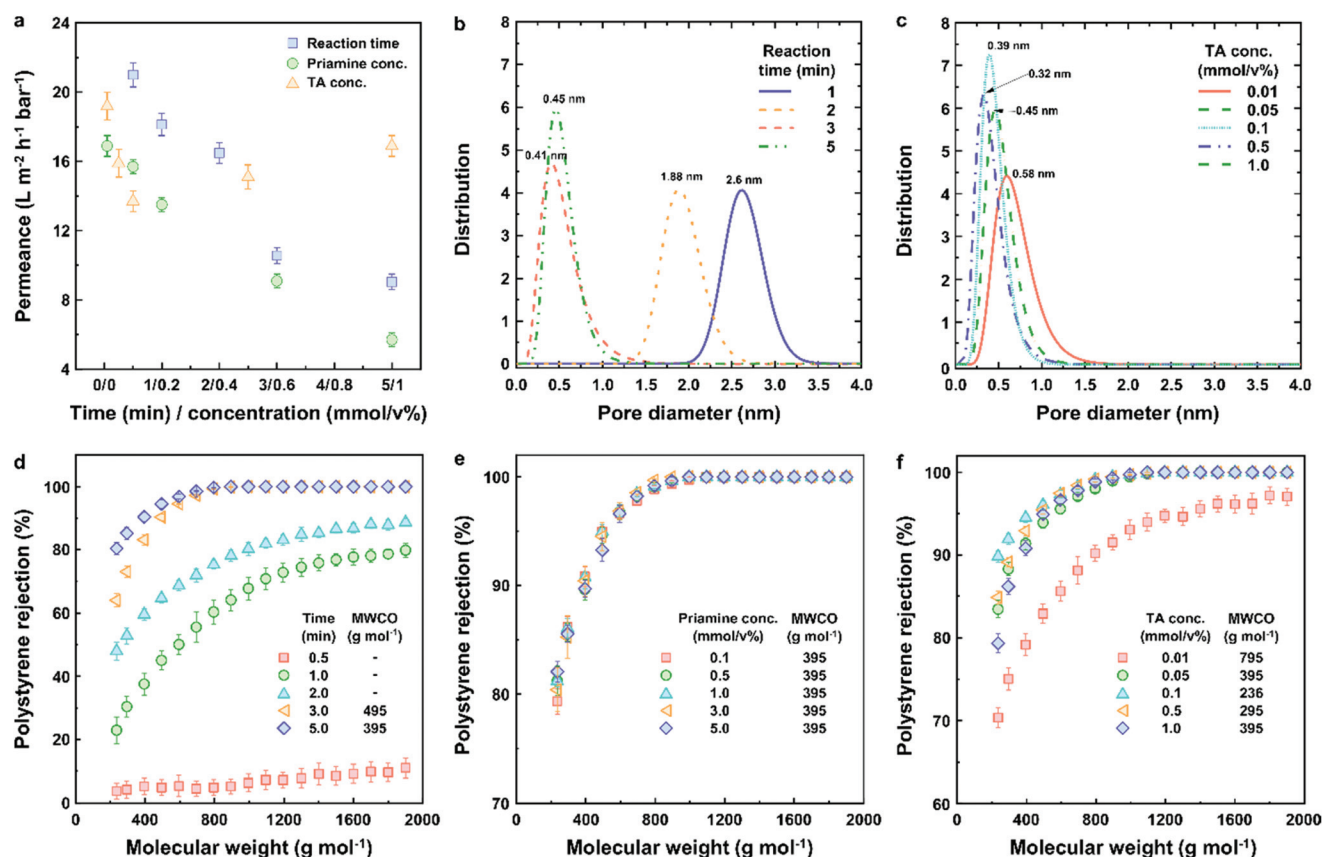
Fig. 3 Membrane separation performance and pore size. (a) Acetone permeance with different reaction times (0–5 min at TA conc. 1.0 mmol/v% and priamine conc. 3.0 mmol/v%), priamine (0–5 mmol/v% at TA conc. 1.0 mmol/v% and 5 min) and TA (0–1 mmol/v% at priamine conc. 0.1 mmol/v% and 5 min) concentrations; pore size with different (b), reaction times and (c), TA concentrations; and the MWCO curves for the TFC membranes prepared with different (d), reaction times, (e), priamine and (f), TA concentrations.

235 g mol^{-1} (Fig. 3a and f). This phenomenon was caused by the formation of a tight chemical structure of the selective layer. Further increase in TA concentration increased both the acetone permeance and MWCO, due to the decrease in density of the chemical structure of the selective layer, which was supported by the change in pore size (Fig. 3c). Therefore, the highest performance membrane with excellent acetone permeance (13.7 L m^{-2} h^{-1} bar^{-1}) and lowest MWCO (235 g mol^{-1}) was achieved at 0.1 mmol/v% of priamine and 0.1 mmol/v% of TA concentrations, indicating that the optimum molar ratio for the IP reaction between priamine and TA is 1.

To assess the improvement of the separation performance of the green TFC membranes, their permeance and rejection were compared with those from the published literature (Fig. 4). The permeance of solvents with a varying polarity exhibited a linear correlation with the solubility parameter (Fig. 4a), which comprises the solvent solubility ($\delta_{p,s}$), viscosity (η) and molar diameter ($d_{m,s}$).[26] The green TFC membrane was found stable in acetone, n-heptane, EtOH, MEK, toluene and MeCN (Fig. S10†). The membrane exhibited similar acetone

and MeCN permeance, and higher permeance of n-heptane, toluene, EtOH, and especially MEK, compared to the TFC on the x-PI membrane in the literature.[26] We assume that the hydrophobic nature of the selective layer led to an increase in the solvent solubility of the membrane surface, which in turn enhanced the permeance. The acetone permeance as a function of styrene dimer rejection for the green TFC membranes was compared with that of the reported integrally skinned asymmetric (ISA), mixed matrix membrane (MMM) and TFC membranes in the literature (Fig. 4b).[27,28] With the change in the priamine and TA monomer concentrations, a performance trade-off was observed, which provided a new upper-bound. Owing to the hydrophobicity of the selective layer, the membrane performance in toluene and n-heptane was found to be competitive with the state-of-the-art petrochemical-based TFC membranes in the literature (Fig. 4c).[29–31]

In order to demonstrate the industrial viability of the green TFC membranes, their long-term performance in hydrophobic solvents was evaluated using a cross-flow nanofiltration rig under continuous operation over 7 days (Fig. 4d). An initial membrane compaction was observed over the first 24 h, which
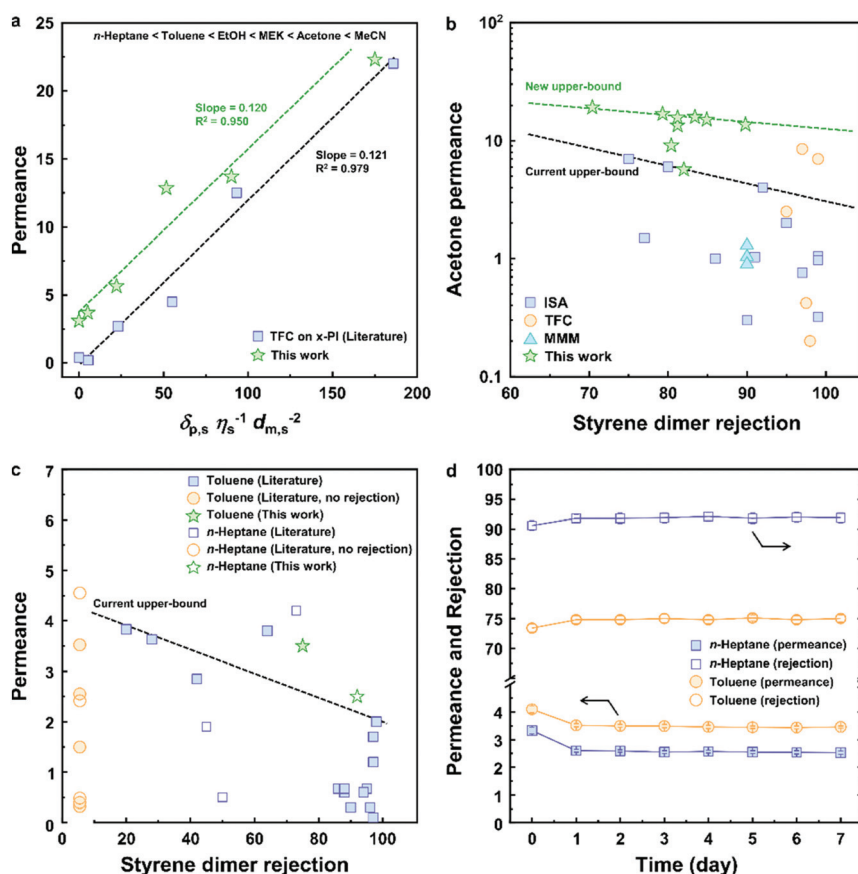
Fig. 4 Comparison of separation performance. (a) Pure solvent permeance as a function of solubility parameter, compared with x-PI comprising MPD and TMC (Table S3†),[26] (b) acetone permeance *versus* styrene dimer (235 g mol^{-1}) rejection, compared with the published literature,[27,28] (c) toluene and n-heptane permeance and styrene dimer rejection, compared with the published literature (Table S4†);[3,8,9,32,33] (d) long-term stability in hydrophobic solvents under continuous operation in cross-flow mode. Permeance and rejection are expressed in L m^{-2} h^{-1} bar^{-1} and percentage, respectively.

manifested in a 1.6 ± 0.2% increase in rejection and 18 ± 3% decrease in permeance. The membrane exhibited a stable steady state performance over the following 6 days of continuous operation. Overall, the outstanding performance and the long-term performance stability demonstrated the potential of green TFC membranes to replace petroleum-based membranes in OSN applications.

Sustainability evaluation

In this work, we have exploited plant-based priamine and TA to produce the selective layer of the TFC membrane on a recycled porous PET support; we successfully performed the IP reaction in green solvents, namely water and *p*-cymene. This is the first report on TFC membranes using natural compounds for both monomers and the solvent system. To evaluate the sustainability of the green TFC membrane, the total number of moles for the monomers and additives used in the fabrication of the selective layer was calculated, and compared with the reported literature (Fig. 5). We found the total mole number for our green TFC membranes to be between 0.11 and 6.0 mmol, and the membrane with an optimum monomer concentration of 0.2 mmol. The common petroleum-based TFC membranes prepared from MPD and TMC, without additives showed the total mole number to be within the 12–34 mmol range (Fig. 5a). The use of additives such as co-solvents and salts significantly increased the total number of moles up to 66 mmol. The existing green TFC literature focused on replacing either one of the monomers or the

solvent to a green alternative. These membranes still used undesired petrochemical-based acyl chlorides or diamines. Seven of them had a greater total mole number than our green TFC membrane, whereas two were comparable.[14,34] We also calculated the chemical and solvent consumption per unit area of membrane (Table S9†). Our green TFC membrane can be fabricated using moles of chemicals 2.7–41 times less than other reported green and petroleum-based TFC membranes.

The hazard and toxicity associated with the IP reaction were investigated through the pictograms of the Globally Harmonized System of Classification and Labeling of Chemicals (Fig. 5c).[35,36] The size of the pictogram for each component was calculated, based on their total mole number. Both the number and the size of pictograms for our green TFC membrane were smaller than those of the TFC membranes prepared by green- and petroleum-based monomers in the published literature. Therefore, the sustainability of our green TFC membrane prepared from TA and priamine was significantly improved by minimizing its toxicity and environmental burden. In addition, a less toxic solvent (*p*-cymene)[21] was used for the fabrication process, in replacement of conventional solvents such as toluene and hexane. The assumptions made when comparing the sustainability of our green TFC membranes with conventional ones highlight the need for future research to report the concentration of monomers and volume of solvents per unit membrane area. This will allow us to make a direct and accurate comparison of the different studies on

Fig. 5 Sustainability analysis of TFC membrane fabrication. Total mole number of the used monomers and additives in the IP process for the reported (a), petroleum-based TFCs (listed in Table S5) and (b), green TFCs (Table S7†); (c), chemical hazards and toxicity associated with TFC membranes (listed in Tables S6 and S8†). The area of a pictogram is proportional to the total mole number of the corresponding chemicals used. The references in the panels can be found in the corresponding tables in the ESI.†

this topic, and ultimately contribute to the progress in the green TFC field.

Conclusions

The challenge of developing green TFC membranes is multi-faceted and lies in finding sufficiently reactive natural monomers that are soluble in green solvents with opposing polarities. The work reported here demonstrates the successful development of hydrophobic thin-film nanocomposite membranes, *via* interfacial polymerization, using solely naturally occurring compounds. Priamine and tannic acid were used as monomers, and *p*-cymene and water were used as solvents. A chemically stable selective layer on the top of a recycled porous poly(ethylene terephthalate) support was rapidly fabricated at room temperature, through the Schiff-base and Michael-addition reactions between the monomers. The produced membranes showed outstanding permeance in six solvents covering a wide range of polarities, and a high styrene dimer rejection due to the hydrophobic nature and ultra-thin thickness (∼30 nm) of the selective layer. This new method provides a new platform for fabricating next-generation OSN membranes, using eco-friendly and abundant natural resources as monomers.

Experimental

Materials

Priamine 1071 and tannic acid (TA, ACS grade) monomers were provided by Croda and Sigma Aldrich, respectively. *p*-Cymene (99%) was purchased from Acros Organics. Acetone (ACS reagent, 99.5%), *n*-heptane (ReagentPlus, 99%), toluene (ACS reagent, 99.5%), ethanol (EtOH, 200 proof, anhydrous, 99.5%), and methyl ethyl ketone (MEK, Emplura 99%) were purchased from Sigma-Aldrich. Acetonitrile (MeCN, HPLC gradient 99.9%). All chemicals were used as received, without any further purification. Type II deionized water with a resistivity of 18.2 MΩ cm at 25 °C (Milli-Q) was used throughout all experiments.

Membrane fabrication

A green TFC membrane was prepared *via* the IP reaction of TA and priamine (Fig. 1a). A recycled PET porous support[20] with an area of approx. 50 cm^2 was immersed in 50 mL of a 0.1 mmol/v% aqueous TA solution for 5 min at laboratory temperature (21 ± 1 °C). The excess solution on the support surface was removed using a rubber roller, followed by an immediate immersion in 50 mL of a 0.1 mmol/v% priamine in *p*-cymene solution for 5 min to enable the formation of the selective layer on the support. The produced membranes were washed three times with *p*-cymene to terminate the IP reaction, followed by drying for 10 min at room temperature. They were stored in DI water containing 1% acetonitrile to prevent bacterial growth. To optimize the performance of the membranes, the reaction time

(0.5, 1, 2, 3 and 5 min), priamine concentrations (0.1, 0.5, 1, 3 and 5 mmol/v%) and TA concentrations (0.01, 0.05, 0.1, 0.5 and 1 mmol/v%) were systemically changed, as shown in Table S1.† In addition, the priamine/TA free-standing film was prepared at a 0.1 mmol/v% monomer concentrations.

Characterization

One dimensional ^{13}C CP/MAS solid-state nuclear magnetic resonance (NMR) spectra were recorded on a Bruker AVANCE III spectrometer operating at 400 MHz resonance frequency, and the following sequence was used: 900 pulses on the proton (pulse length 2.4 s), then a cross-polarization step with a contact time of typically 2 ms, and finally the acquisition of the ^{13}C NMR signal under high power proton decoupling. The delay between the scans was set to 4 s to allow the complete relaxation of the 1H nuclei; the number of scans ranged from 3000 to 10 000. An exponential apodization function corresponding to a line broadening of 80 Hz was applied, prior to the Fourier transformation. X-ray photoelectron spectroscopy (XPS, Axis Supra, Kratos) analysis was performed on a Kratos Axis Supra instrument equipped with a monochromatic Al Kα X-ray source ($h\nu$ = 1486.6 eV) operating at a power of 150 W and under UHV conditions in the range of ∼10^{-9} mbar. All spectra were recorded in hybrid mode, using electrostatic and magnetic lenses and an aperture slot of 300 μm × 700 μm. The wide and high-resolution spectra were acquired at fixed analyzer pass energies of 80 eV and 20 eV, respectively. The samples were mounted in floating mode in order to avoid differential charging. The high-resolution peaks were deconvoluted using a XPSPEAK 4.1 software program. Attenuated total-reflectance Fourier-transform infrared (ATR FT-IR, Nicolet is 10, Thermo Fisher Scientific) spectroscopy was used to investigate the chemical bonding and shift of the film and monomers. The dried membrane samples were cut in liquid nitrogen, using a blade for cross-sectional imaging and sputter-coated with iridium (a thickness of 5 nm) to avoid any charging of the sample. Surface and cross-sectional images of membranes were recorded using a scanning electron microscope (SEM, Merlin, ZEISS). The thickness of the selective layer was calculated from the cross-sectional images of the membranes. In addition, the layer thickness was double-checked using atomic force microscopy (AFM, Dimension icon, Veeco), after placing the layer on a silicon-wafer. The 3D topography of all membranes was collected by AFM, in the tapping mode, using a cantilever (RTESPA, Bruker) with a scan area of 5 μm × 5 μm, and scan rate of 0.7 Hz. Three different positions on each sample surface were scanned to obtain the average arithmetic roughness (R_a) values with the standard deviation. The water contact angle of membranes was measured by the sessile drop method using a drop shape analyzer (Easy drop, KRUSS) equipped with a video camera. The average values were obtained from at least five measurements for each sample.

Membrane separation

The organic solvent nanofiltration performance of the TFC membranes was evaluated using a crossflow membrane separ-

ation rig. An ATEX-rated gear pump manufactured by MSE Ltd (UK) was used for the recirculation of the retentate stream set to 1200 mL min⁻¹. The membranes were rinsed with the solvent of the filtration, and then stored in the solvent for 24 h prior to the filtration. To reach a steady-state operation, the membranes were conditioned under 10 bar for 24 h, prior to the permeance and rejection measurements. The permeance (eqn (1)) was obtained by measuring the permeate volume (V) over a given time (t) period, and a given membrane area ($A = 52$ cm²) and applied pressure.

$$\text{Permeance}[\text{L m}^{-2}\,\text{h}^{-1}\,\text{bar}^{-1}] = \frac{J}{\Delta P} = \frac{V}{\Delta P \times A \times t} \qquad (1)$$

The rejection profiles were determined from the ratio of the permeate (c_{permeate}) and retentate ($c_{\text{retentate}}$) concentrations of the solutes. Standard polystyrene markers containing 1 g L⁻¹ PS580 and PS1300 and 0.1 g L⁻¹ methyl styrene dimer (236 g mol⁻¹) were used for the filtrations in toluene. Owing to the very low solubility of the markers in n-heptane, the concentrations were only 10 ppm each, and required a 1% toluene additive. Molecular weight cut-off (MWCO), defined as the lowest molecular weight solute in which 90% of it is retained by the membrane, was estimated from the rejection curves by linear interpolation. Two independent measurements were performed on independently prepared membranes; the standard deviations are reported in the figures.

$$\text{Rejection}[\%] = \left(1 - \frac{c_{\text{permeate}}}{c_{\text{retentate}}}\right) \times 100 \qquad (2)$$

Sustainability analysis

The mole number of each monomer or additive was calculated per 100 mL of the solvent used in the IP process. The total mole number is the sum of the mole number for each monomer and additive. In addition, to evaluate the chemical hazards and toxicity of the petroleum-based and green TFC membranes, the total mole number was converted to the area of a pictogram provided by the Globally Harmonized System of Classification and Labeling of Chemicals.[34,35] The same volume of solution for each monomer and the same area of membrane were used in the IP process because most of the literature describes only the monomer concentration without the solution volume and/or the membrane area.

Author contributions

Sang-Hee Park: Conceptualization, Methodology, Validation, Formal analysis, Investigation, Data curation, Writing – original draft, Review & editing, and Visualization; Abdulaziz Alammar: Methodology and Investigation; Zsolt Fulop: Investigation and Visualization; Bruno A. Pulido: Data curation; Suzana P. Nunes: Supervision, Resources and Review & editing; Gyorgy Szekely: Conceptualization, Methodology, Writing – review & editing, Supervision, Resources, Funding acquisition and Project administration.

Conflicts of interest

The authors declare no competing interest.

Acknowledgements

References

1 S.-H. Park, S. J. Kwon, M. G. Shin, M. S. Park, J. S. Lee, C. H. Park, H. Park and J.-H. Lee, Polyethylene-supported high performance reverse osmosis membranes with enhanced mechanical and chemical durability, *Desalination*, 2018, **436**, 28–38.

2 G. M. Geise, H.-S. Lee, D. J. Miller, B. D. Freeman, J. E. McGrath and D. R. Paul, Water purification by membranes: The role of polymer science, *J. Polym. Sci., Part B: Polym. Phys.*, 2010, **48**, 1685–1718.

3 M. F. Jimenez-Solomon, Y. Bhole and A. G. Livingston, High flux membranes for organic solvent nanofiltration (OSN) – Interfacial polymerization with solvent activation, *J. Membr. Sci.*, 2012, **423–424**, 371–382.

4 V. Freger, Nanoscale heterogeneity of polyamide membranes formed by interfacial polymerization, *Langmuir*, 2003, **19**, 4791–4797.

5 L. Li, S. Zhang and X. Zhang, Preparation and characterization of poly(piperazineamide) composite nanofiltration membrane by interfacial polymerization of 3,3′,5,5′-biphenyl tetraacyl chloride and piperazine, *J. Membr. Sci.*, 2009, **335**, 133–139.

6 S.-H. Park, S. O. Hwang, T.-S. Kim, A. Cho, S. J. Kwon, K. T. Kim, H.-D. Park and J.-H. Lee, Triclosan-immobilized polyamide thin film composite membranes with enhanced biofouling resistance, *Appl. Surf. Sci.*, 2018, **443**, 458–466.

7 M. F. Jimenez-Solomon, P. Gorgojo, M. Munoz-Ibanez and A. G. Livingston, Beneath the surface: Influence of supports on thin film composite membranes by interfacial polymerization for organic solvent nanofiltration, *J. Membr. Sci.*, 2013, **448**, 102–113.

8 M. F. Jimenez-Solomon, Y. Bhole and A. G. Livingston, High flux hydrophobic membranes for organic solvent nanofiltration (OSN) – Interfacial polymerization, surface modification and solvent activation, *J. Membr. Sci.*, 2013, **434**, 193–203.

9 H. Zhang, Y. Zhang, L. Li, S. Zhao, H. Ni, S. Cao and J. Wang, Cross-linked polyacrylonitrile/polyethyleneimine-

polydimethylsiloxane composite membrane for solvent resistance nanofiltration, *Chem. Eng. Sci.*, 2014, **106**, 157–166.

10 B. Li, Y. Cui and T.-S. Chung, Hydrophobic, perfluoropolyether-coated thin-film composite membranes for organic solvent nanofiltration, *ACS Appl. Polym. Mater.*, 2019, **1**, 472–481.

11 V. Froidevaux, C. Negrell, S. Caillol, J.-P. Pascault and B. Boutevin, Biobased amines: From synthesis to polymers; Present and Future, *Chem. Rev.*, 2016, **116**, 14181–14224.

12 M. Wloch, J. Datta and K. Blazek, The effect of high molecular weight bio-based diamine derivative of dimerized fatty acids obtained from vegetable oils on the structure, morphology and selected properties of poly(ether-urethane-urea)s, *J. Polym. Environ.*, 2018, **26**, 1592–1604.

13 G. Schmidt, J. T. Woods, L. X.-B. Fung, C. J. Gilpin, B. R. Hamaker and J. J. Wilker, Strong adhesive from corn protein and tannic acid, *Adv. Sustainable Syst.*, 2019, **3**, 1900077.

14 L. Perez-Manriquez, P. Neelakanda and K.-V. Peinemann, Tannin-based, thin-film composite membranes for solvent nanofiltration, *J. Membr. Sci.*, 2017, **541**, 137–142.

15 M. He, H. Sun, H. Sun, X. Yang, P. Li and Q. J. Niu, Non-organic solvent prepared nanofiltration composite membrane from natural product tannin acid (TA) and cyclohexane-1,4-diamine (CHD), *Sep. Purif. Tech.*, 2019, **223**, 250–259.

16 Q. Wei, K. Achazi, H. Liebe, A. Schulz, P. M. Noeske, I. Grunwald and R. Haag, Mussel-inspired dendritic polymers as universal multifunctional coatings, *Angew. Chem., Int. Ed.*, 2014, **53**, 11650–11655.

17 Q. Li, Z. Liao, X. Fang, D. Wang, J. Xie, X. Sun, L. Wang and J. Li, Tannic acid-polyethyleneimine crosslinked loose nanofiltration membrane for dye/salt mixture separation, *J. Membr. Sci.*, 2019, **584**, 324–332.

18 Plastic upcycling, *Nat. Catal.*, 2019, **2**, 945–946, DOI: 10.1038/s41929-019-0391-7.

19 A. Rahimi and J. M. Garcia, Chemical recycling of waste plastics for new materials production, *Nat. Rev. Chem.*, 2017, **1**, 1–11.

20 B. A. Pulido, O. S. Habboub, S. L. Aristizabal, G. Szekely and S. P. Nunes, Recycled poly(ethylene terephthalate) for high temperature solvent resistant membranes, *ACS Appl. Polym. Mater.*, 2019, **1**, 2379–2387.

21 C. M. Alder, J. D. Hayler, R. K. Henderson, A. M. Redman, L. Shukla, L. E. Shuster and H. F. Sneddon, Updating and further expanding GSK's solvent sustainability guide, *Green Chem.*, 2016, **18**, 3879–3890.

22 Z. Wang, S. Zhao, R. Song, W. Zhang, S. Zhang and J. Li, The synergy between natural polyphenol-inspired catechol moieties and plant protein-derived bio-adhesive enhances the wet bonding strength, *Sci. Rep.*, 2017, **7**, 1–10.

23 X. Zhang, M. D. Do, P. Casey, A. Sulistio, G. G. Qiao, L. Lundin, P. Lillford and S. Kosaraju, Chemical modification of gelatin by a natural phenolic cross-linker, tannic acid, *J. Agric. Food Chem.*, 2010, **58**, 6809–6815.

24 M.-Y. Lim, Y.-S. Choi, J. Kim, K. Kim, H. Shin, J.-J. Kim, D. M. Shin and J.-C. Lee, Cross-linked graphene oxide membrane having high ion selectivity and antibacterial activity prepared using tannic acid-functionalized graphene oxide and polyethyleneimine, *J. Membr. Sci.*, 2017, **521**, 1–9.

25 X. Li, B. Chen, W. Cai, T. Wang, Z. Wu and J. Li, Highly stable PDMS-PTFPMS/PVDF OSN membranes for hexane recovery during vegetable oil production, *RSC Adv.*, 2017, **7**, 11381–11388.

26 S. Karan, Z. Jiang and A. G. Livingston, Sub-10 nm polyamide nanofilms with ultrafast solvent transport for molecular separation, *Science*, 2015, **348**, 1347–1351.

27 M. F. Jimenez-solomon, Q. Song, K. E. Jelfs, M. Munoz-Ibanez and A. G. Livingston, Polymer nanofilms with enhanced microporosity by interfacial polymerization, *Nat. Mater.*, 2016, **15**, 760–767.

28 P. Marchetti, M. F. Jimenez-Solomon, G. Szekely and A. G. Livingston, Molecular separation with organic solvent nanofiltration: A critical review, *Chem. Rev.*, 2014, **114**, 10735–10806.

29 S. Darvishmanesh, A. Buekenhoudt, J. Degreve and B. V. Bruggen, General model for prediction of solvent permeation through organic and inorganic solvent resistant nanofiltration membranes, *J. Membr. Sci.*, 2009, **334**, 43–49.

30 S. Hermans, H. Marien, C. V. Goethem and I. F. J. Vankelecom, Recent developments in thin film (nano)composite membranes for solvent resistant nanofiltration, *Curr. Opin. Chem. Eng.*, 2015, **8**, 45–54.

31 S. R. Hosseinabadi, K. Wyns, V. Meynen, R. Carleer, P. Adriaensens, A. Buekenhoudt and B. V. Bruggen, Organic solvent nanofiltration with Grignard functionalized ceramic nanofiltration membranes, *J. Membr. Sci.*, 2014, **454**, 496–504.

32 D. Fritsch, P. Merten, K. Heinrich, M. Lazar and M. Priske, High performance organic solvent nanofiltration membranes: Development and thorough testing of thin film composite membranes made of polymers of intrinsic microporosity (PIMs), *J. Membr. Sci.*, 2012, **401–402**, 222–231.

33 H. Siddique, L. G. Peeva, K. Stoikos, G. Pasparakis, M. Vamvakaki and A. G. Livingston, Membranes for organic solvent nanofiltration based on preassembled nanoparticles, *Ind. Eng. Chem. Res.*, 2013, **52**, 1109–1121.

34 Y. Zhang, Y. Su, J. Peng, X. Zhao, J. Liu, J. Zhao and Z. Jiang, Composite nanofiltration membranes prepared by interfacial polymerization with natural material tannic acid and trimesoly chloride, *J. Membr. Sci.*, 2013, **429**, 235–242.

35 T. V. T. Phan, C. Gallardo and J. Mane, Green motion: A new and easy to use green chemistry metric from laboratories to industry, *Green Chem.*, 2015, **17**, 2846–2852.

36 L. Cseri and G. Szekely, Towards cleaner PolarClean: Efficient synthesis and extended applications of the polar aprotic solvent methyl 5-(dimethylamino)-2-methyl-5-oxopentanoate, *Green Chem.*, 2019, **21**, 4178–4188.